Time-Based Competition in Multistage Manufacturing: Stream-of-Variation Analysis (SOVA) Methodology—Review

D. CEGLAREK   darek@engr.wisc.edu
W. HUANG   huang@cae.wisc.edu
S. ZHOU   szhou@engr.wisc.edu
Department of Industrial Engineering, University of Wisconsin-Madison, Madison, WI 53706-1572, USA

Y. DING   YuDing@iemail.tamu.edu
Department of Industrial Engineering, Texas A&M University, College Station, TX 77843, USA

R. KUMAR   kumarr@3dcs.com
Y. ZHOU   yzhou@3dcs.com
Dimensional Control Systems, Inc., Troy, MI 48084, USA

Abstract. Frequency of model change and the vast amounts of time and cost required to make a changeover, also called time-based competition, has become a characteristic feature of modern manufacturing and new product development in automotive, aerospace, and other industries. This paper discusses the concept of time-based competition in manufacturing and design based on a review of on-going research related to stream-of-variation (SOVA or SoV) methodology. The SOVA methodology focuses on the development of modeling, analysis, and control of dimensional variation in complex multistage assembly processes (MAP) such as the automotive, aerospace, appliance, and electronics industries. The presented methodology can help in eliminating costly trial-and-error fine-tuning of new-product assembly processes attributable to unforeseen dimensional errors throughout the assembly process from design through ramp-up and production. Implemented during the product design phase, the method will produce math-based predictions of potential downstream assembly problems, based on evaluations of the design and a large array of process variables. By integrating product and process design in a pre-production simulation, SOVA can head off individual assembly errors that contribute to an accumulating set of dimensional variations, which ultimately result in out-of-tolerance parts and products. Once in the ramp-up stage of production, SOVA will be able to compare predicted misalignments with actual measurements to determine the degree of mismatch in the assemblies, diagnose the root causes of errors, isolate the sources from other assembly steps, and then, on the basis of the SOVA model and product measurements, recommend solutions.

Key Words: variation reduction, quality, root cause identification, manufacturing systems

1. Introduction: Time-based-competition—New paradigm and challenges

The US automotive industry has dominated world auto markets for years. The mass production paradigm, initiated by Henry Ford and Frederick W. Taylor, has been the most powerful tool for the United States in global markets for almost half of the last century. However, the landscape has shifted dramatically from the old world of mass production, which was characterized by few standardized products, homogeneous markets, and long product life

cycle and development lead time. A new standard is gradually emerging in which increased customization, product proliferation, heterogeneous markets, shorter product life cycle and development time, responsiveness, and related factors are increasingly becoming key features (Bollinger, 1998; Gervin and Barrowman, 2002). For example, in Japan, Toyota was reportedly offering customers five-day delivery from the time the customer designed a customized car on a CAD system (from modular options) to the actual product delivery.

One of the characteristic features of the automotive industry is the frequency of model change and vast amounts of time and cost that are required to make a changeover. This trend has continuously gone up in the last two decades. Since 1980s, US car market's total demand has essentially remained stable, but the number of nameplates has increased by 35% from 139 to 183, respectively. This increase continued during the 1990s essentially creating a paradigm shift in automotive industry.

The newly emerging manufacturing paradigm is characterized by the so-called time-based-competition (TBC). The time to market for a new product or the service responsiveness of a company has become the new cutting edge in global market competition (Ulrich, Sartorius, Pearson, and Jakiela, 1993). The major advantages of this new strategy are widely recognized to be (1) use of a newer technology than competitors in a newly developed product (2) capturing new market niche earlier than that of a competitor (3) higher customer satisfaction, and (4) better integration of the entire enterprise. In addition, it is possible that the company will parallelly achieve higher quality, lower cost, and a leaner organization (Suri, 1998).

In order to support as well as take full advantage of the aforementioned TBC strategies, new techniques such as quick response manufacturing (Suri, 1998), reconfigurable manufacturing system (Koren et al., 1999; Mehrabi, Ulsoy, and Koren, 2000), agile manufacturing etc. have been proposed, developed, and applied in the last decade.

1.1.   Challenges in automotive industry

Due to rapid changes in market demands in recent years, shortened product cycle is inevitably becoming the prevailing trend. For example, in the automotive industry, a product life cycle will be shortened to 2–3 years in a few years as compared to the current 4–7 years and 9–12 years from a few years ago. Additionally, market requirements demand significantly shorter new product realization cycles. Currently, it takes 24 months for the world's top auto manufacturers to develop a new car, with development time expected to be reduced to 12–18 months within the next five years. Similar trends are also apparent in the appliance and consumer good industries. As a result, there are a number of new concepts in the area of production system development, such as flexible and reconfigurable manufacturing systems (RMS) and quick response manufacturing (QRM), which are increasingly being adopted in industrial practices. However, due to lack of confidence in predicting system performance (ramp-up time, expected yield, and relatively long time necessary to reach it), there is tremendous resistance to implement advanced technology or innovations in new product/process development (CIRP, 2000).

The most significant obstacles toward reducing new product realization time stem from the complexity of the product/process and knowledge- or expertise-based product/process

development methods. They can be further categorized into (1) *design phase*: large number of design/engineering changes that have to be made after the product has been designed and at times even after it has been built (6,000 changes on average for a new automotive body development); (2) *pre-production phase*: long ramp up time, especially for complex systems such as flexible machining transfer lines (up to 12–14 months), and automotive assembly lines (3–5 months); (3) *full production phase*: low production yield (below design intent expectations: 65–70% for flexible machining line).

1.1.1. Product/process design phase. Each new automobile design has a unique body architecture with a typical market life cycle of about 4–7 years. The assembly systems to produce these vehicles are also traditionally unique designs that are based on the constraints of product. When new models are introduced, very little of the old assembly system can be salvaged for a new product, thus, resulting in expending resources for a new body architecture, new assembly systems and new facilities. This development process is shown in Figure 1. To satisfy the ever-increasing demands in product variety, quality, and delivery time, both the body assembly system development time and launch time must be shrunk significantly.
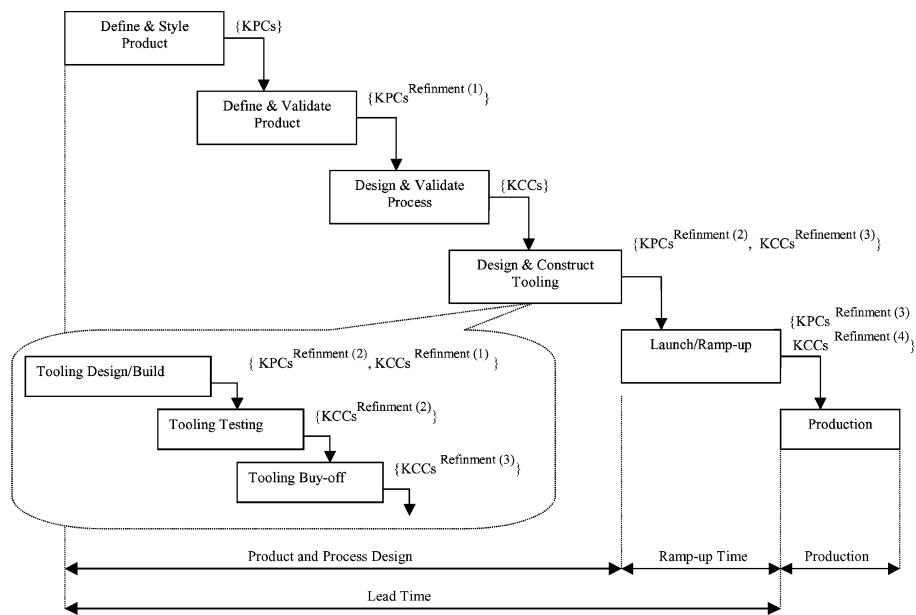
{KPCs} – set of Key Product Characteristics (KPCs)
{KCCs} – set of Key Control Characteristics (KCCs) [Process characteristics]
$KCC^{Refinment (1),(2),(3),(4)}$ – number of stages of process development which requires engineering changes of KCC

*Figure 1.* Manufacturing system development stages.

Product development time strongly depends on the ratio of "first time right" strategy, which tries to eliminate additional changes after the design phase.

For example, according to a 1999 survey conducted by the University of Michigan, it is estimated that some US automotive manufacturers reach 50–60% of "first time right" during design stage, as compared to 80% achieved by the top international competitor. This causes significant barriers in realizing TBC manufacturing strategies in the overall product development cycle (Thomke and Fujimoto, 2000).

Additionally, it was reported that in aerospace and automotive industries 67–70% of all design changes are related to product-dimensional variation (Shalon, Gossard, Ulrich, and Fitzpatrick, 1992; Ceglarek and Shi, 1995) caused by lack of technology for accurate prediction of process performance/variation during the product/process design. It is widely recognized that geometrical accuracy and dimensional variation are two of the most important quality and productivity factors in many manufacturing processes. In fact, dimensional variation is introduced into virtually every design when manufactured (Parkinson, Sorensen, and Pourhassan, 1993). Thus, the lack of a comprehensive technology for product/process performance prediction and control is a major barrier to further progress in new product and process development. Moreover, the waste resulted from the aforementioned engineering changes done after the design phase can be translated into $84/vehicle for repair/rework (this does not include process change costs and overhead cost), lower production yield, and delay in starting production (higher product development cost, lost market share due to delay in introduction of a new product, shorter production time—overall lower profits or higher product costs).

1.1.2. Ramp-up for new production systems.

New production ramp-up/launch time is critical in new product manufacturing. The major efforts during ramp-up are focused on identifying the root causes of process variation (Figure 2). However, current industrial practice in ramp-up time reduction is far less than satisfactory. For example, in one US automotive plant the designed production volume was reached near full after 14 months of launching a new vehicle assembly line. Most of the problems are related to dimensional control of product variation. In another plant, the design intended yield could not be maintained due to dimensional variation of parts after 6 months of product launch (ERC-RMS, 1999; Figure 3).

Although product and process design impact one another, product design has traditionally been separated from process design even in different companies, for example, tooling wherein dies, fixtures, material handling facilities etc. are usually designed and manufactured by different suppliers. Lately, manufacturers have begun to investigate ways to simultaneously evaluate product designs and manufacturing processes in an attempt to eliminate downstream problems of manufacturing (ramp-up time, yield etc.) (El-Gizawy, Hwang, and Brewer, 1990; Gadh, 1993). However, most of the design rules and guidelines require experience-based knowledge—there was no generic model, which could lead to comprehensive technology to solve the aforementioned problems. Traditionally, design engineers have arrived at a product design configuration through use of engineering science principles. This often results in the designer specifying the target values for critical design parameters.
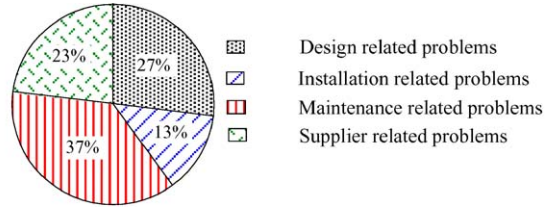
(a) Classification of dimensional fault root causes
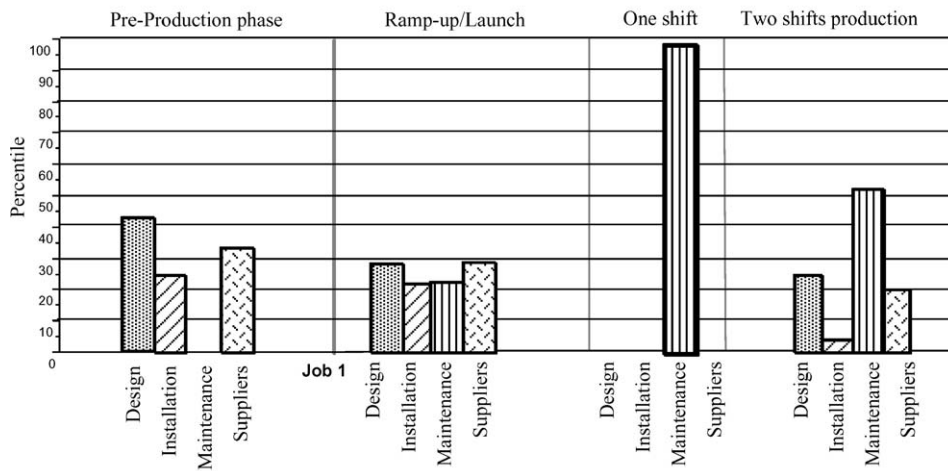
(b) Fault root cause classification during different product/process development phases

Figure 2. Dimensional fault root cause classification during ramp-up and full production (Ceglarek and Shi, 1995).
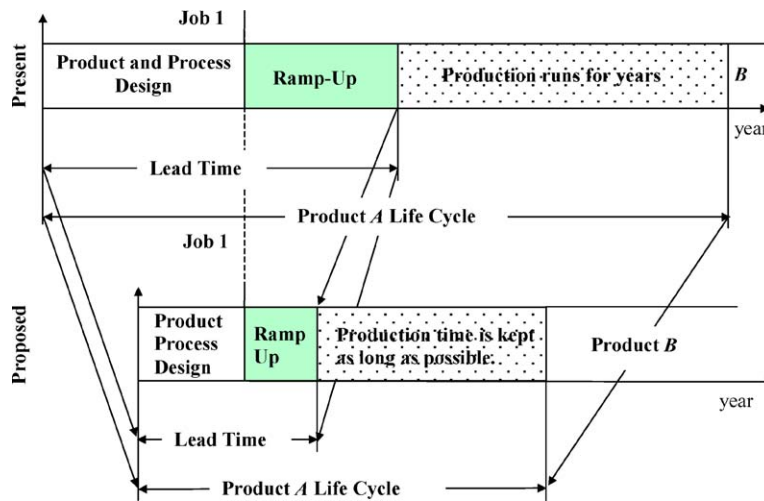

Figure 3. New product/process development flow diagram (Koren et al., 1999).

However, through this procedure, the specification limits are usually determined by the design engineer before the final product is released for production. This *product-oriented* approach is referred to as *over-the-wall* design since there is no systematic integration of design and manufacturing. This out-of-date design philosophy is one of the reasons why some auto companies still have a lower first-time-right rate. A typical example is tolerance design.

Traditional tolerancing research (Chase and Parkinson, 1991) mainly focused on an assembly that is built up through numerous mating features of individual components. In other words, the traditional tolerancing technique is primarily concerned with dimensional or geometrical variables of a component in an assembly. Traditional tolerancing techniques can be labeled as *product-oriented tolerancing*, since the explicit inclusion of process information in the traditional tolerancing scenario is limited, where product variables and manufacturing process are only weakly connected by the associated manufacturing cost. As long as the cost-tolerance function is specified, tolerance allocation can be conducted based on the mathematical/functional model without considering any other effects from the manufacturing process. Recently, researchers have come to realize that the traditional product-oriented approach overlooks the impact of *process variables*, such as information regarding fixture and tooling configuration, on product quality in complex multistage manufacturing processes. The quality of the final product from a multistage manufacturing process is not only determined by the tolerance of each individual component but also affected by variations of numerous process variables such as fixturing error, force, and tooling vibration during different manufacturing stages. The term "process variable" covers a very broad category and includes rather diverse number of parameters associated with manufacturing process. They are not part of the product information but indicators of process status. One of the major challenges in analyzing process variables is that the relationship between the variation of process variable and product quality is very complex, depending on process design, tooling layout, and manufacturing sequence among others. Moreover, additional complexity is introduced because process variables can change over time due to factors such as tooling degradation. Hence, they cannot be represented by simple worst case or root square sum stack-up models or product functional model with only kinematic relationship.

1.2. New Strategy: Introduction to stream-of-variation analysis (SOVA)

Manufacturers in the 21st century will face frequent and unpredictable market changes. These changes include rapid-frequency introduction of new products, increased demand for new products and mix of products, new parts for existing products, and overall new process technologies. To gain the competitive advantage, manufacturing companies must be able to analyze, predict and optimize manufacturing system performance during the design phase (that is, do all design in the first time right "FTR[Design]" approach) and be able to identify and isolate root causes of all faults during ramp-up time (do all fault isolation in the first time right "FTR[Diagnosis]" approach).

This leads to a new manufacturing strategy namely, math-based SOVA system working in "FTR[Design/Diagnose]" mode for product/process performance analysis. In the last decade,
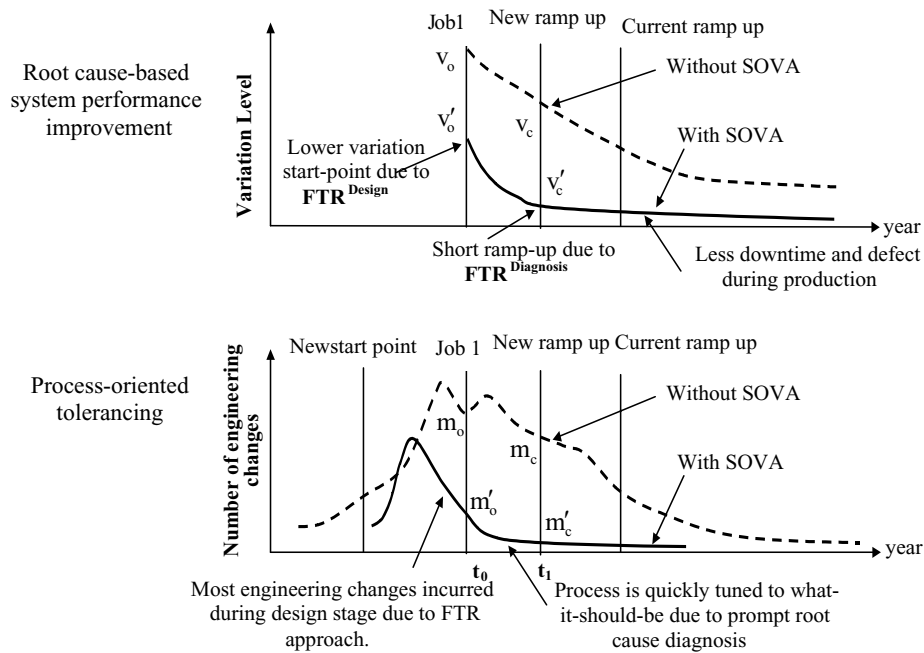
Figure 4. New product/process development criteria and requirements.

the so-called stream of variation analysis (SOVA) methodology has been proposed and developed to overcome the aforementioned challenges (Ceglarek and Shi, 1994, 1995, 1996; Apley and Shi, 1998; Hu, 1997; Ding, Ceglarek, and Shi, 2000, 2002a, 2002b; Ding, Shi, and Ceglarek, 2002c). SOVA is a generic math model for variation propagation analysis in multistage manufacturing systems. SOVA integrates multivariate statistics, control theory as well as design/manufacturing knowledge (CAD/CAM models) into a unified framework. SOVA serves two objectives (Figure 4):

- In the *design phase*, the SOVA can be used for analysis, prediction, and optimization of manufacturing system performance following the concept of "FTR$^{\text{Design}}$". Given the process and tooling design information, SOVA can simulate the variation propagating throughout the process and then predict the final product-dimensional variation and resultant product geometry.
- In the production *ramp-up phase*, SOVA can be used to identify and isolate fault root causes following the concept of "FTR$^{\text{Diagnosis}}$". Given the process and tooling design information, SOVA can demonstrate high responsiveness in identifying and isolating root causes of dimensional variation, that is, identifying the most severe dimensional faults, localizing the critical stations contributing most to the final product variation and speedily isolating the root causes of dimensional faults—achieving faster required V_c' level of variation as shown in Figures 4 and 5.
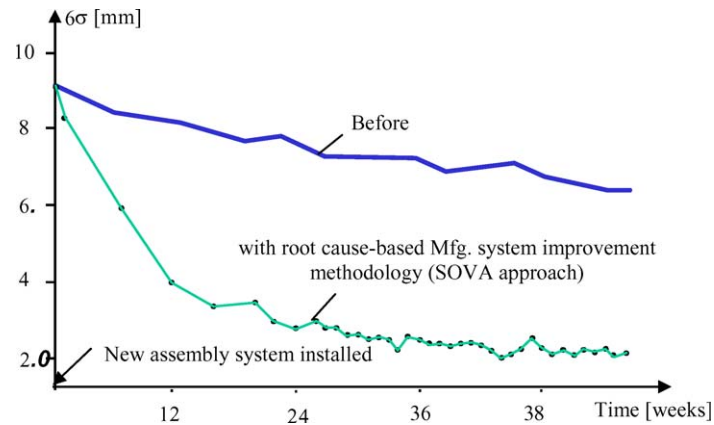
Figure 5.   Variation level comparative evaluation (Ceglarek and Shi, 1995; ERC-RMS, 1999).

Figure 6.   Automotive body at the optical measurement station.

2.   Background on automotive assembly process

Geometrical relations dominate assembly of the automotive body, shown in Figures 6 and 7, such that the quality of the assembly process can be determined by the dimensional integrity of a product. This indicates that the level of product-dimensional variation can be a critical index for final evaluation of the assembled vehicle.

2.1.   Product and process

An automotive body is built from sheet metal parts, which have different shapes, sizes, and thickness, depending on their functions. These parts are categorized as structural or nonstructural. Structural parts support the automotive body structures and includes (1) main parts, such as rails and plenum, or (2) reinforcement parts, for instance, door hinge
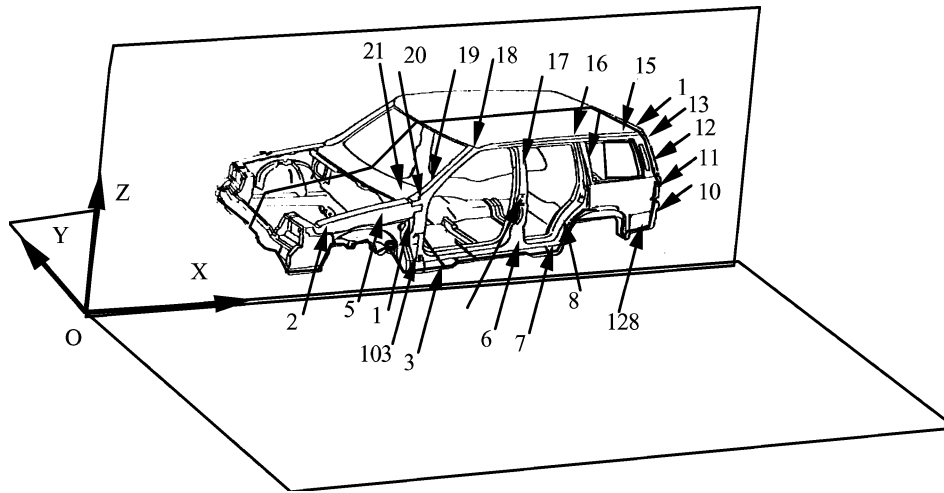
Figure 7. The body coordinate system with an example of sensor locations.

reinforcements. Nonstructural parts include door outer, cowl-side, roof and so on. Based on the research conducted by Takezawa (1980) and Ceglarek (1994), one can conclude that structural parts, mainly due to their greater rigidity, have a much bigger impact on automotive body dimensional accuracy than nonstructural parts.

The automotive body assembly process includes three major elements: (1) assembly fixtures (2) welding robots or welding guns, and (3) part handling mechanisms. These three elements conduct three major functions of the assembly process: part positioning/holding, part joining, and part/subassembly transfer.

On a typical plant floor, these elements are linked into assembly lines dominated by part positioning and welding stations. Each assembly line produces a major subassembly or final product. There are usually two types of lines: (1) component subassembly lines, and (2) framing assembly lines. The component subassembly lines include underbody line, and two aperture (side frames) lines—left and right hand. The major element of the framing line is an automotive body framing station, where underbody, apertures, and roof bows are joined together. Figure 8 shows an outline of an assembly line with descriptions of the geometrical stations in the framing line. The framing station is marked as S_3. In general, all stations can be divided into geometrical and re-spot stations. The geometrical stations handle parts with position-setting mechanical jigs designed for each type of vehicle. The part is set in position by these dedicated jigs, initially welded and then transferred to a re-spot station for final welding. During the re-spot operations, robots add welding spots to the parts to increase their strength. Usually, re-spot stations do not affect the position or orientation of the part or subassembly. The geometrical stations have a much larger impact on the dimensional variation of the product than re-spot stations.

The total number of geometrical stations varies from process to process. On average, at least 25–35 geometrical stations and no less than 30–40 re-spot stations assemble an automotive body made of 150 to 250 sheet metal parts.
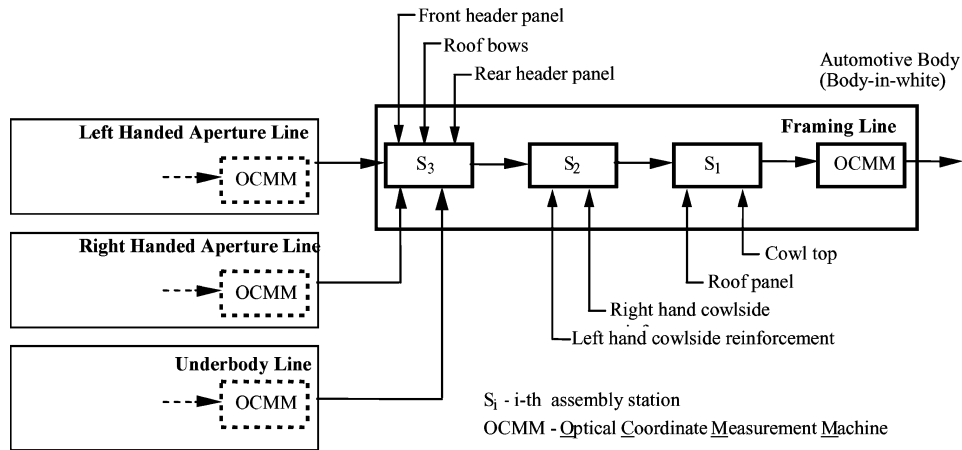
Figure 8.   Outline of the assembly process: critical stations of the framing line.

The major function of the assembly station is to correctly position parts before the start of welding operations. The usual method of positioning stamped parts is based on the 3-2-1 layout principle. However, during studies of actual assembly processes, it was also noted that an n-2-1 layout principle, where $n > 3$ is often used. The selection of the part locating principle depends on the size and rigidity of the part (Menassa and DeVries, 1989; Cai, Hu, and Yuan, 1996), and directly affects inherent level of product-dimensional variation. Part transport to and from stations is accomplished by many different mechanisms such as electrified monorails, tip-up drives, and so on.

2.2.   Measurement

Modern dimensional diagnosis of the automotive body requires accurate data to satisfy quality assurance requirements. Currently, three measurement gages are most often used for checking part/subassembly dimensions: (1) hard gage fixtures and layout plates, (2) coordinate measuring machines (CMMs), and (3) optical coordinate measuring machines (OCMMs; Figure 6). CMMs and OCMMs are currently widely applied to collect coordinate data or KCCs (key control characteristics) on a sampled auto body for quality control and diagnosis purposes.

2.2.1. CMM.   Introduced in the 1960s, CMMs are very accurate and flexible. They allow for measurements at selected points on the part with an accuracy of 0.01 mm. Their flexibility is based on their capacity for quick reprogramming measurement cycles when checking different parts or points. The drawback of CMMs is the time lag before receiving measurement information. An automotive body must be taken off-line and transferred to the CMM room for measurement. A fully operational CMM can measure up to eight automotive bodies during an eight-hour shift. The results from the CMM are useful for assessing the final quality of an automotive body or subassemblies.

2.2.2. OCMM (Figure 6). In recent years, the implementation of the in-line optical co-ordinate measurement machine (OCMM) in automotive industry has provided new oppor-tunities for automotive body assembly diagnosis. OCMMs are installed in-line at the end of major assembly processes, such as framing, side frames, underbody, etc. (Figure 8). Each OCMM consists of several laser sensors allowing for noncontact measurement of a body or subassembly relative to design nominal. On average, the measurement cycle takes a few seconds, with accuracy around 0.25 mm, and static and dynamic repeatabil-ity within 6-σ equal to 0.14 and 0.25 mm, respectively (Perceptron, 1991). The OCMM gage measures from 100 to 150 points on each major assembly with 100% sample rate. As a result, the OCMM provides a tremendous amount of dimensional information, which can be used for assembly process control. All OCMMs in the plant use the same coordi-nate system, called the body coordinate system, because it is easy to use and compares data from different gages. Figure 7 shows the coordinate axes and reference points in the body coordinate system. The principles of the measurement sensors are described by Greer (1988), and the outline of the sensor setup for automotive body assembly can be found in Hu (1990).

2.3. Product development phases

A characteristic feature of the automotive industry is the frequency of model changes and the vast amounts of time and labor required to make a changeover. The automotive body assembly is regarded as the least flexible process in the overall vehicle assembly (Sekine, Koyama, and Imazu, 1991). During a model change, tooling must be changed to match the newly established process and product design. Given the complexity of this process, the automotive body development cycle requires three to four years of lead time. Even the final stage of the automotive body development cycle, after vehicle and hard tooling are designed, lasts for about a year. This final stage includes the following phases: (1) pilot program, (2) prevolume production, (3) launch, and (4) full production. These phases are described below, focusing on the dimensional issues.

The pilot program starts when prototype vehicles are built to verify manufacturing pro-cesses after 100% of the vehicle dimensions and tolerances are approved. The pilot program is the first phase, beginning on average five months ahead of the launch. It includes (a) verify-ing the designed KCC (key control characteristics; locators and clamps positions) schemes for tooling fixtures during the assembly process; and (b) setting the process capability of the designed tooling.

Prevolume production starts 1–2 months ahead of launch, after the tooling is set up at the assembly plant. The goal of prevolume production is to validate process capability and initially identify the sources of variation.

After determining that the vehicle can reach acceptable quality levels, the launch phase follows. Typically, at launch phase, a number of problems must still be resolved before a vehicle of desired quality level can be built. The length of the launch phase depends on how quickly dimensional problems can be resolved while simultaneously speeding up production rate. Identification of dimensional faults becomes one of the bottlenecks in reaching full production rate.
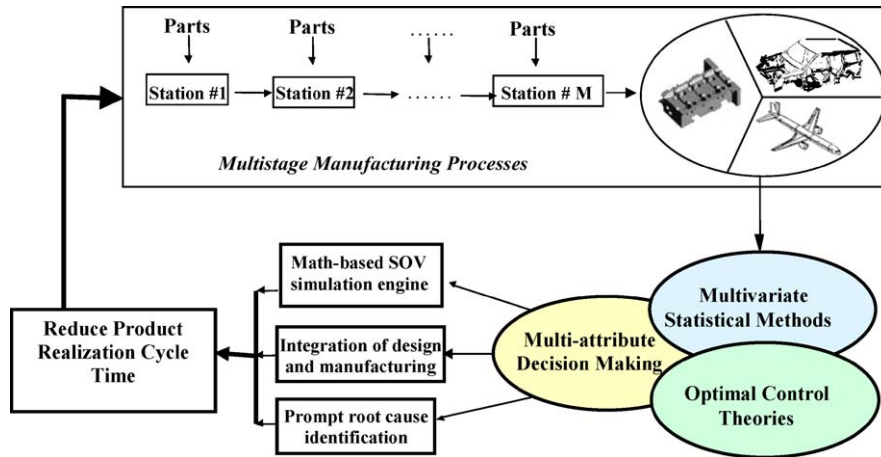
Figure 9.   Multidisciplinary nature of the SOVA research.

The full production phase begins after the production rate reaches the assigned level with acceptable quality. Typically, at this phase, assembly line maintenance issues and product quality assurance requirements become dominant.

3.   Stream-of-variation analysis methodology

The stream of variation analysis (SOVA or SoV) methodology is a generic simulation engine for modeling, analysis, and performance prediction of multistage manufacturing processes where product geometry and dimensional variation are of critical importance (Figures 9 and 10). An example is in machining dedicated/flexible transfer lines and/or assembly lines used in automotive, aerospace, or appliance industries. The SOVA system is based on a math-based unified representation (state-space model) of the multistage manufacturing processes. This generic math-based state space representation allows for integration of key process and product characteristics (KPC—key product characteristics, KCC—key control characteristics) represented in CAD/CAM models, with information about process layout, sequence of operations, and production system observability (allocation of measurement gages and position of measurement points for quality check).

A *math-based state space model* has been used as a framework to describe process deviation and variation propagation at both single station and multistation system/process levels. Based on this model, advanced control theory and statistics are used for optimized process control and quality improvements (Figure 9) in both development and production phases.

3.1.   State space model of variation propagation

A multi-station assembly process of an automotive body assembly is described in detail in Ceglarek, Shi, and Wu (1994), Jin and Shi (1999) and Ding et al. (2000). The modeling
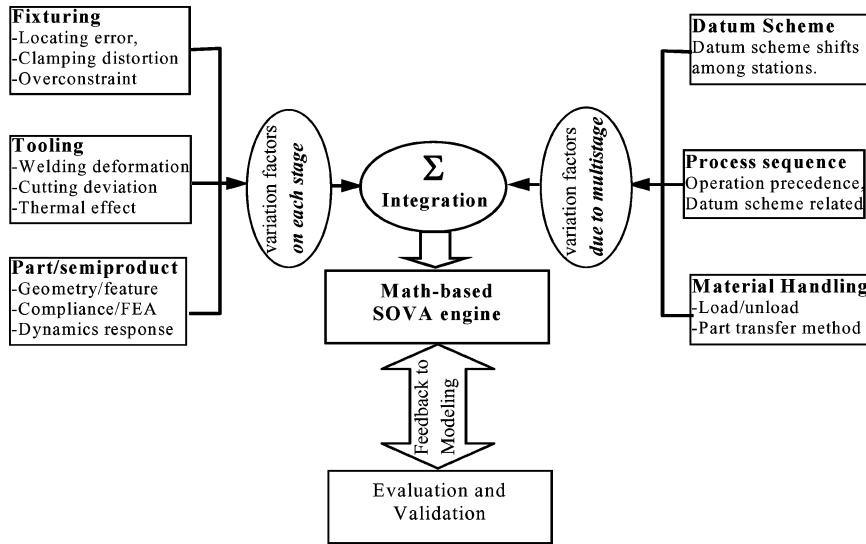
Figure 10. Modeling of SOVA in manufacturing processes.

of fixture-related variation propagation in such an assembly process has been studied by Mantripragada and Whitney (1999), Jin and Shi (1999), Lawless, Mackay, and Robinson (1999), Ding et al. (2000), and Camelio, Hu, and Ceglarek (2003). For purposes of illustration, an example of state space modeling for automobile body assembly is presented below which accounts for two major variation contributors. These two factors are fixture variation at each single station (Figure 11(a)), where $\delta P_2(z)$ is the deviation in Z-direction at locator P_2; and station-to-station correlation errors or the reorientation-induced variation when an assembly is transferred to another station (Figure 11(b)).

A multistage assembly system (Figure 12) is composed of a series of single stations. The variation propagation throughout the entire system can be modeled by using a state
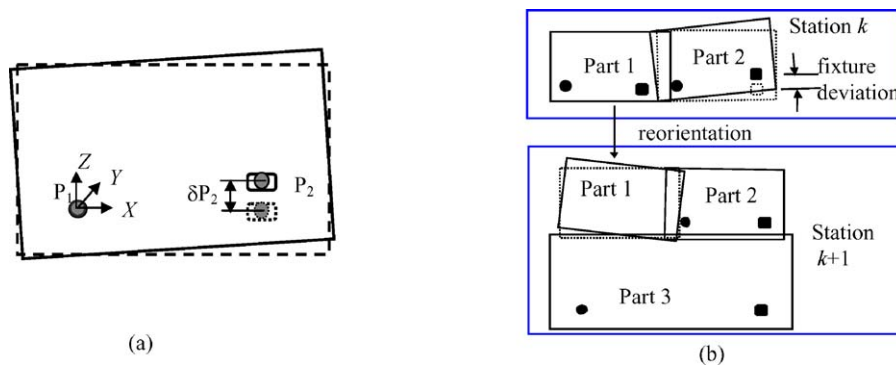

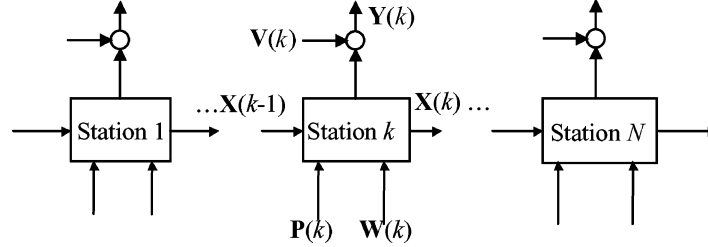*Figure 11.* Variation induced at a single station and across stations.

Figure 12.   Diagram of an assembly process with *N* stations.

space representation (Jin and Shi, 1999; Ding et al., 2000; Camelio et al., 2003). The state vector describes the geometrical errors of all relevant components in the system. Similar to a sequential dynamic system, this specific state space model uses a station index to replace the time index in a traditional state space model. The state space transfer or the transmitted relations between stations can thus be set up as the following two equations:

$$\mathbf{X}(k) = \mathbf{A}(k-1)\mathbf{X}(k-1) + \mathbf{B}(k)\mathbf{U}(k) + \mathbf{W}(k), \tag{1}$$

$$\mathbf{Y}(k) = \mathbf{C}(k)\mathbf{X}(k) + \mathbf{V}(k), \tag{2}$$

where $\mathbf{X}(k)$ is the state vector or product quality information (e.g., part dimensional deviations) after operations at station k. $\mathbf{U}(k)$ stands for the process variation contributed at station k. Product measurements of key product characteristics (KPC) at station k are included in $\mathbf{Y}(k)$, and $\mathbf{W}(k)$ and $\mathbf{V}(k)$ are unmodeled errors and sensor noise, respectively. Matrices $\mathbf{A}(k)$ and $\mathbf{B}(k)$ in the above model include information regarding process design such as fixture layout on individual station k and the change of fixture layouts (datum transfer) across stations, and $\mathbf{C}(k)$ includes sensor placement information (the number and location of sensors on station k). The corresponding physical interpretation of $\mathbf{A}$, $\mathbf{B}$, and $\mathbf{C}$ is presented in Table 1, where $\boldsymbol{\Phi}(k, j) \equiv \mathbf{A}(k-1) \cdots \mathbf{A}(j)$ and $\boldsymbol{\Phi}(j, j) \equiv \mathbf{I}$, and the detailed expression

Table 1.   Interpretation of system matrices.

Symbol	Name	Relationship	Interpretation	Assembly task
$\mathbf{A}$	Dynamic matrix	$\mathbf{X}(k-1) \xrightarrow{\mathbf{A}(k-1)} \mathbf{X}(k)$	Change of fixture layout between two adjacent stations	Assembly transfer
$\boldsymbol{\Phi}(k, i)$	State transition matrix	$\mathbf{X}(i) \xrightarrow{\boldsymbol{\Phi}(k,i)} \mathbf{X}(k)$	Change of fixture layout among multiple stations	Assembly transfer
$\mathbf{B}$	Input matrix	$\mathbf{U}(k) \xrightarrow{\mathbf{B}(k)} \mathbf{X}(k)$	Fixture layout at station k	Part positioning
$\mathbf{C}$	Observation matrix	$\mathbf{X}(k) \xrightarrow{\mathbf{C}(k)} \mathbf{Y}(k)$	Sensor layout at station k	Inspection

can be found in Ding et al. (2000). Suppose there is only end-of-line observation, that is, $k = N$ in the observation equation of equation (2). Then, we have

$$\mathbf{Y}(N) = \sum_{k=1}^{N} \mathbf{C}(N)\mathbf{\Phi}(N, k)\mathbf{B}(k)\mathbf{U}(k) + \mathbf{C}(N)\mathbf{\Phi}(N, 0)\mathbf{X}(0) + \varepsilon. \tag{3}$$

Here, $\mathbf{X}(0)$ corresponds to the initial condition, resulting from imperfectly manufactured stamped parts, and ε is the summation of all modeling uncertainty and sensor noise terms. Moreover, it was assumed that this process involves sheet metal assembly with only lap-lap joint and thus, the stamping imperfection of part dimensions will not affect the propagation of variations (Ceglarek and Shi, 1998). Then, we can set initial conditions to zero. The uncertainty term ε can be neglected in the design stage.

The variation propagation can then be approximated as

$$\mathbf{K}_Y = \sum_{k=1}^{N} \boldsymbol{\gamma}(k)\mathbf{K}_U(k)\boldsymbol{\gamma}^T(k), \tag{4}$$

where $\mathbf{K}_Y$ and $\mathbf{K}_U(k)$ represent the covariance matrices of $\mathbf{Y}(N)$ and $\mathbf{U}(k)$, respectively, and $\boldsymbol{\gamma}(k) = \mathbf{C}(N)\mathbf{\Phi}(N, k)\mathbf{B}(k)$. Thus, product quality is affected by $\mathbf{K}_U(k)$, the covariance of process variables. Based on the engineering knowledge, it is known that process variable in this problem is related to fixturing error at every assembly station, which is often caused by the clearance of locating pinhole pairs.

4. Applications

4.1. Fixture fault diagnosis in manufacturing phase

This section will deal with the application of the state space model for fixture faults diagnosis in multistage manufacturing system (MMS). The propagation of deviation in an N-station MMS can be represented in the form of state space equations (1) and (2), where $k \subset 1, 2, \ldots, N$. Unmodeled noises $\mathbf{V}$ and $\mathbf{W}$ are assumed to be mutually independent. These definitions follow the same notation as used in Ding et al. (2000). Matrices $\mathbf{A}$, $\mathbf{B}$, and $\mathbf{C}$ encode the design information of process configuration.

Equation (1) implies that part deviation at station i is influenced by two sources: the accumulated part deviation up to station $i - 1$, and the deviation contributed at the current station. Equation (2) is the observation equation. If sensors are installed at one or more stations in a production line, the index for the observation equation is actually a subset of $\{1, 2, \ldots, N\}$, whereas the index for the state equation is the complete set.

Assume that the end-of-line sensing strategy, the most commonly used sensor installation scheme in industrial setting, is employed. End-of-line sensing means that observation is only available at the last station N, that is, $k = N$ for equation (2), and

$$\mathbf{Y} = \mathbf{C}\mathbf{X}(N) + \mathbf{V} \tag{5}$$

where $\mathbf{Y} \in \mathbf{R}^{q \times 1}$ indicates that q measurements are obtained at station N. The indices for $\mathbf{Y}$, $\mathbf{C}$, and $\mathbf{W}$ are dropped since they are all Ns. The input–output relationship can be represented as

$$\mathbf{Y} = \sum_{k=1}^{N} \gamma(k)\mathbf{U}(k) + \gamma(0)\mathbf{X}(0) + \varepsilon. \tag{6}$$

Here, $\mathbf{X}(0)$, $\mathbf{W}$, $\mathbf{V}$ are the basic random variables in a stochastic process and thus, usually assumed to be independent. The assumption can be partially released to include the situation where the basic random variables are dependent by enlarging the state vector. Moreover, $\mathbf{U}$, the fixturing deviations at station k, are independent with those basic random variables as well since only an open loop system is now being considered. Given the independent relationships between these variables, the input–output covariance relationship can be obtained from equation (6) to characterize the variation propagation in a production line,

$$\mathbf{K}_Y = \sum_{k=1}^{N} \gamma(k)\mathbf{K}_U(k)\gamma^T(k) + \gamma(0)\mathbf{K}_0\gamma^T(0) + \mathbf{K}_\varepsilon, \tag{7}$$

where $\mathbf{K}_Y$ represents the covariance matrix of random vector $\mathbf{Y}$, and $\mathbf{K}_0$ is given as the initial variability condition. $\mathbf{K}_\varepsilon$ can be estimated from the data when no fixture fault was present.

It is assumed that only the lap joints are involved in the current model, implying that fabrication imperfection of parts will not affect the propagation of variations. Thus, it is reasonable to set the initial condition $\mathbf{K}_0$ to zero. The process can then be approximated as follows:

$$\mathbf{K}_Y = \sum_{k=1}^{N} \gamma(k)\mathbf{K}_U(k)\gamma^T(k) + \mathbf{K}_\varepsilon. \tag{8}$$

This equation suggests that while being contaminated by noise, the variation of the final product is mainly the contribution of variations of fixturing errors at all stations.

Without considering the matrix $\mathbf{K}_\varepsilon$, we have

$$\mathbf{K}_Y^0 = \sum_{k=1}^{N} \gamma(k)\mathbf{K}_U(k)\gamma^T(k).$$

It has been proven by Ceglarek and Shi (1996) and Ding et al. (2002b) that the eigenvalue–eigenvector pair $\{\lambda_{kp}, \gamma_p(k)\}$ of matrix $\mathbf{K}_Y^0$ can be used for fixture fault diagnosis, λ_{kp} represents the variance of the principal component at station k caused by fault p. The eigenvector is the pattern vector of this fixture fault, manifesting the fixturing variation by generating a mode shape of measurement vector $\mathbf{Y}$. In the rest of this paper, assume $\gamma_p(k)$ as a normalized eigenvector using the Euclidean norm.

The basic concept of the diagnostic methodology is shown in Figure 13. If a fault of fixture element (locator) exists in a station, a symptom will be reflected in the final product
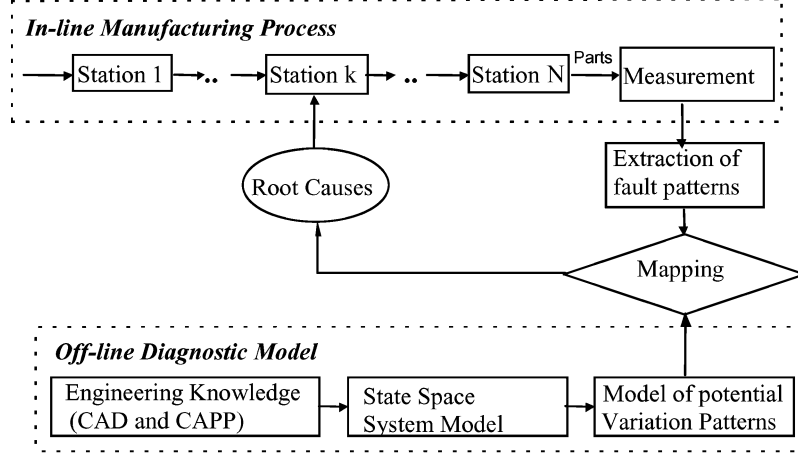
Figure 13. Outline of the diagnostic methodology.

or downstream intermediate products. From off-line CAD information and the state space model, a set of all possible fault patterns can be generated. Measurement data are collected in-line (OCMM) and analyzed using one of the multivariate statistical methods, for example, the principal component analysis (PCA), to extract the fault feature patterns. Fault isolation can then be conducted by mapping the feature patterns of real production data with predetermined fault patterns generated from the analytical model. This can be done by calculating the similarity of the two patterns. The similarity of any two pattern vectors $\gamma_p(i)$ and $\gamma_q(k)$ is defined as the acute angle formed by fault pattern vectors

$$\theta_{pq}(i,k) = \cos^{-1}\langle\gamma_p(i), \gamma_q(k)\rangle, \quad 0 \le \theta \le \frac{\pi}{2},$$

where $\langle\cdot, \cdot\rangle$ represents the inner product of two vectors. The least acute angle between measured pattern vector and one of the potential fault pattern vector reveals the most likely fault and its location. It is obvious that if the least angle between any pair of possible fault patterns is too small then they may not be easily distinguishable under the contamination of possible noises, so that the similarity analysis has to be done before diagnosis.

4.1.1. Case study. A multistage process is set up, which is abstracted from a side aperture assembly line in the automotive industry, including three assembly stations and one measurement station. The final product is made of four parts, as shown in Figure 14.

The assembly sequence and datum shift scheme regarding this assembly process are shown in Figure 15. $\{\{P_1, P_2\}, \{P_3, P_4\}\}$ denotes the locating pairs used at station 1, with $\{P_1, P_2\}$ and $\{P_3, P_4\}$ depicting the first and the second parts, respectively. The others are
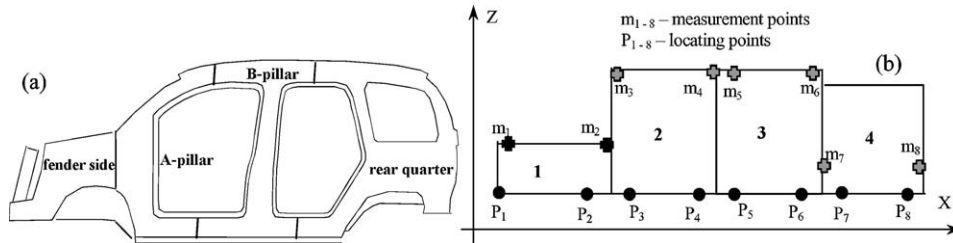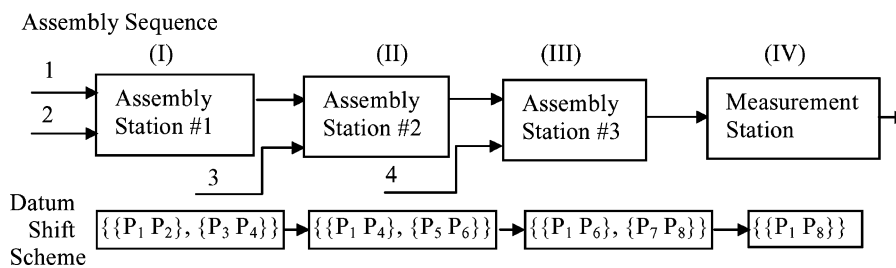
Figure 14. Geometry of the assembly.

Figure 15. Assembly sequence and datum shift scheme.

similarly defined. At station 4, which is the measurement station, one pair of locating pins $\{P_1, P_8\}$ is used since there is only one piece of the assembly to measure.

As shown in Figure 14(b), part motion in both X and Z directions are controlled by 4-way pins of P_1, P_3, P_5, and P_7 and in the Z direction by 2-way pins of P_2, P_4, P_6, and P_8. It is also assumed that the fixture error at the measurement station can be neglected when compared with assembly fixtures. The relationship between fault indices and root causes on each station is shown in Table 2 and in Figure 16.

As indicated in Figure 14(b), there are two sensors on each part at the last station (end-of-line sensing). Each sensor can measure part deviation in both X and Z directions. Two sensors are sufficient to detect the deviation in position and orientation of a 2D rigid part. The angles (in degree) between all fault pattern vectors at station i are listed as follows, where $p, q = 1, 2, 3, 4, 5, 6$. Since these matrices are symmetric, only the upper half is

Table 2. Fault indices and their root causes.

| Index	Fault root cause	Index	Fault root cause
$p = 1$	4-way pin on the 1st part/subassembly is faulty in X-direction	$p = 4$	4-way pin on the 2nd part/subassembly is faulty in X-direction
$p = 2$	4-way pin on the 1st part/subassembly is faulty in Z-direction	$p = 5$	4-way pin on the 2nd part/subassembly is faulty in Z-direction
$p = 3$	2-way pin on the 1st part/subassembly is faulty in Z-direction	$p = 6$	2-way pin on the 2nd part/subassembly is faulty in Z-direction
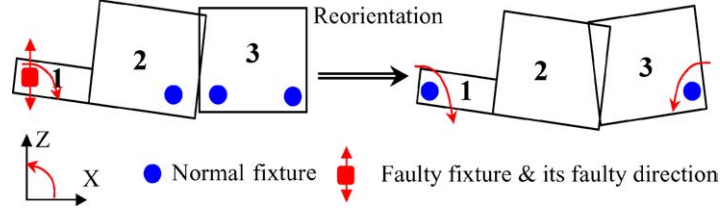
Figure 16. Geometric interpretation of fault $p = 2$ at the 2nd station.

listed.

$$[\theta_{pq}(1, 1)] = \begin{pmatrix} - & 64.0 & 90 & 0 & 45 & 53.4 \\ & - & 38.3 & 64.0 & 51.7 & 19.3 \\ & & - & 90 & 90 & 57.6 \\ & & & - & 45 & 53.4 \\ & & & & - & 32.4 \\ & & & & & - \end{pmatrix}$$

$$[\theta_{pq}(2, 2)] = \begin{pmatrix} - & 53.8 & 90 & 0 & 33.1 & 48.6 \\ & - & 44.9 & 53.8 & 45.1 & 7.27 \\ & & - & 90 & 90 & 52.2 \\ & & & - & 33.1 & 48.6 \\ & & & & - & 37.8 \\ & & & & & - \end{pmatrix} \quad (9)$$

$$[\theta_{pq}(3, 3)] = \begin{pmatrix} - & 82.5 & 90 & 0 & 71.1 & 76.7 \\ & - & 23.6 & 82.5 & 66.4 & 21.7 \\ & & - & 90 & 90 & 45.3 \\ & & & - & 71.1 & 76.7 \\ & & & & - & 44.7 \\ & & & & & - \end{pmatrix}$$

Suppose fault $p = 6$ occurred at the 1st station. The sample covariance matrix $\mathbf{K}_Y$ is calculated by using 500 samples generated by the variation simulation analysis software using Monte Carlo simulations (DCS, 2000). The PCA is performed to get the eigenvalue/eigenvector pairs. The first eigenvalue/eignvector pair is $\lambda_1 = 0.6011$ and

$$\begin{aligned} \gamma_1 = [0.2302 & \quad -0.0713 \quad 0.2178 \quad -0.4484 \quad -0.4054 \quad -0.5858 \quad -0.4230 \\ 0.0736 & \quad -0.0062 \quad 0.0068 \quad 0.0151 \quad -0.0164 \quad 0.0257 \quad 0.0084 \\ 0.0132 & \quad 0.0051]^T. \end{aligned} \quad (10)$$

Table 3. Angle of fault pattern vectors between stations (All values are degrees.)

$\theta(1, 2)$	$\theta(2, 3)$	$\theta(1, 3)$
66.2	54.5	76.4

Table 4. Angle between γ_1 and fault patterns for single fault.

	$P = 1$ or 4	$p = 2$	$p = 3$	$p = 5$	$p = 6$
1st station	54.1	18.2	56.4	33.7	**2.76**
2nd station	89.6	84.1	82.3	89.4	84.8
3rd station	88.4	86.0	86.0	89.1	86.6

The first eigenvalue accounts for 53% of the total variation and is 8.5 times larger than the second largest eigenvalue. The angles between γ_1 and potential fault patterns are listed in Table 4. All units are in degrees (°). The smallest angle indicates the fault. Here it is 2.76° for $p = 6$ at the 1st station. By using within-station fault pattern angles in equation (9) and between-station fault pattern angles in Table 3 we know the angle between fault pattern of $p = 6$ at station 1 and its closest pattern vector is 19.3°. Thus, the fault is considered to be correctly identified.

4.2. *Sensor placement optimization*

A fixture serves to ensure part location and holding (clamping) stability, deterministic part location, and total restraint in car body assembly. To estimate the extent of realization of these desirable characteristics, we characterize the fixture by defining a layout of tooling elements (TE), which include locating pins (P) and block locators with clamps (C). Tooling faults are directly attributable to one or a combination of failure conditions associated with each of the TEs. Such TE fault conditions are, in turn, a direct cause of part mislocation in assembly. TE faults have been found to be of both inherent-in-design and the developed-through-process-life forms. Instances of the former include poor clamp design/manufacture, block locator-clamp mating mismatches and off-dimension locating pins. Failures of the latter form may occur from locator wear, inclusions on and pitting of mating surfaces, and degradation in applied clamp pressure levels due to part fatigue over time.

Efficient fault isolation depends on an effective sensor layout. The configuration of the sensor layout becomes relevant when multiple sensors are used to provide a comprehensive problem description. Multiple sensor usage demands a better strategy on sensor data fusion/integration. In the following analysis a generalized 3-2-1 fixture of Figure 17 is used to demonstrate the method proposed in Khan et al. (1998) and Khan et al. (1999) for optimal placement of sensors. The generalized fixture of Figure 17 provides the basis for the definition of a generic fault type categorization (Figure 18). Each fault pattern presented in Figure 18 can be modeled as eigenvectors of $\mathbf{K}_Y^0$ described in Section 4.1. These fault patterns will be also called diagnostic vectors.

C_1, C_2, C_3 : Block locators constraining Y direction part motion
P_1 : Pin locator constraining X & Z direction part motion
P_2 : Pin locator constraining Z direction part motion
M_1, M_2, M_3 : Candidate Sensor/Measurement locale
Note: Dotted lines represent Control Axes

Note: Dotted lines represent Control Axes.

$M_3(m_{3x}, m_{3y}, m_{3z})$

$P_2(x_{p2}, y_{p2}, z_{p2})$

$C_3(x_{p3}, y_{p3}, z_{p3})$

$M_2(m_{2x}, m_{2y}, m_{2z})$

$C_2(x_{p2}, y_{p2}, z_{p2})$

$P_1(x_{p1}, y_{p1}, z_{p1})$

$C_1(x_{p1}, y_{p1}, z_{p1})$

$M_1(m_{1x}, m_{1y}, m_{1z})$
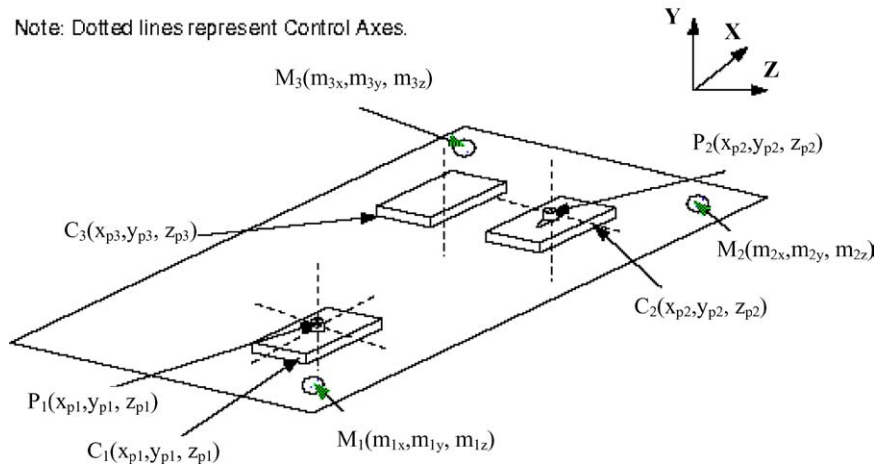
Figure 17.   3-2-1 Fixture layout.

Fault Element	Failure Type	Failure Effect	Fault Manifestation	n_{CTE}	CTE Direction
P_1	Type 2:Failure in Z axis	Rotation		1	Z
P_1	Type 2:Failure in X axis	Rotation		0	-
P_2	Type 3:Failure in Z axis	Rotation		1	Z
C_1	Type 4:Failure in Y axis	Rotation		1	Y
C_2	Type 5:Failure in Y axis	Rotation		1	Y
C_3	Type 6:Failure in Y axis	Rotation		1	Y

n_{CTE} – Number of Tooling Elements (locators) which define the fault variation pattern;

Figure 18.   3-2-1 Fault manifestations (Khan et al., 1999).

An optimal sensor location can be obtained by *maximizing* the *minimum* distance between each pair of dominant eigenvectors of $\mathbf{K}_Y^0$, and obtained for each of the tooling faults. The connotation of the maximization premise is to increase the power, or the degree of reliability, of the discriminant. Here the discriminant serves in a pattern recognition sense, as an estimator of the membership of each observed or hypothesized fault to one of the fault type class. Efficient fault discrimination (diagnosis) is thus possible if the sensor locale provides a maximal spread of fault type classes in space. In the event of sensor noise or multiple fault type coexistence, the primary fault type associated with the prominent eigenvector can be readily distinguished.

Measurements in three axes at each of its three sensor locations provide nine sensor variable measures (Figure 17) and are sufficient to determine the position of a rigid part located by 3-2-1 fixture. A set of *diagnostic* vectors can now be defined as the set of vectors associated with each of these faults for a given tooling configuration (locating layout) and sensor locales. A diagnostic vector

$$\boldsymbol{d}(i) = (d_{1i}, \ldots, d_{ni})^T \tag{11}$$

has n entries (where n is the number of sensor variable measures) describing a variation pattern caused by a type i fault. Elements d_{ji} ($j = 1 \ldots n$) represent a ratio of the standard deviation in a component direction to the overall sensor standard deviation associated with the fault type. If Y_j represents the measured variable, then

$$d_{ji} = \frac{\sigma_{Y_j}}{\sigma} \quad \text{for } j = 1, \ldots, n \tag{12}$$

where σ_{Y_j} is the standard deviation of variable Y_j, and $\sigma = \sqrt{\sum_{j=1}^{n} \sigma_{Y_j}^2}$.

A diagnosability index is proposed which quantifies the ability of the system, with sensors at a candidate sensor locale, to isolate faults. The diagnosability or fault isolation index, J, may be defined as a function of the minimum distance between any two pairs of diagnostic vectors, $\mathbf{d(i)}$ $i=1,\ldots 6$, over all such pairs:

$$J = \forall_{i \neq j} \min \|d(i) - d(j)\|. \tag{13}$$

Thus, the index J is an estimate of the dimensional measure of the closest pairing of fault type manifestations (in fault space) for a candidate sensor locale. The desirability criteria can now be formulated in terms of a search in dimensional space for a sensor locale, which when mapped into fault space, results in the maximization of J. The $\{\mathbf{d(i)}, \mathbf{d(j)}\}$ pair, corresponding to the smallest Euclidean distance measure, varies during the iterative search procedure. This represents a search for the "maximal spread" referred to earlier. The problem may be succinctly formulated as a constrained optimization, where the objective function is sought to be maximized subject to inequality constraints:

$$J_{\text{opt}} = \forall_{i \neq j} \max[\min W_{ij} \|d(i) - d(j)\|] \quad \text{s.t.} G(x, y, z) \leq 0. \tag{14}$$

$G(x, y, z)$ represents the constraint condition set on sensor locations corresponding to "blacked-out" areas on the fixture or part. Thus, constraints formulated from CAD data directly reflect positions on the fixture, which for a number of reasons may be infeasible as a candidate sensor locale. The proposed optimization is generic to 3-2-1 fixtures; weights W_{ij} are introduced to provide fixture-specific control on the relevance of specific tooling faults to the fixture under consideration. These may take on binary (1/0) values, to reflect the absence of a certain fault type in a configuration; r real values, to represent the relative importance of the detection of a certain fault type, constituting a *design for diagnosis*. This design approach complements design for the fundamental function of part positioning, accomplished through conventional TE selection, to ensure a stable part location. To provide an optimal level of detectability, an optimal *sensor locale plan* is then incorporated into the design, using the designed TE locations to guarantee the best level of fault detection and isolation. By utilizing the J_{opt} index, the spread and location of the **d(i)** are optimized to obtain such a locale. Optimization on the J_{opt} index is implemented using a set of functions from the Matlab toolbox, implementing a sequential quadratic programming method. The optimization performance of the functions is seen to be robust to changes of initial conditions. The further extension of the above methodology is presented in Ding, Kim, Ceglarek, and Jin (2003) and in Huang, Kong, Ceglarek, and Brahmst (2004).

4.3. *Process design evaluation.*

One of the critical indicators of process performance—product geometrical quality (dimensional variation)—is used in the following analysis for process design evaluation. Product quality is characterized by dimensional variation of critical design features that affect both product functionality and levels of customer satisfaction. In automotive industry, these critical design features are known as KPCs (key product characteristics). The KPCs are controlled during the assembly process by fixtures locators and clamps (TEs—tooling elements) known as KCCs (key control characteristics). The KCCs are critical dimensional control characteristics for product positioning and thus, are the determining factors in achieving the required dimensional accuracy of KPCs. In a multistation process, the impact of KCCs' variation on KPC's dimensional accuracy depends on process design configuration including the geometry of fixture locating layout on every station and the station-to-station locating layout change. Early design evaluation of multistation assembly processes is very important for new product development and also for designing a robust manufacturing system to improve product quality.

The state space model can provide the basis for process design evaluation in the following ways (Ding et al., 2002a): (i) the variation propagation model, as shown in equation (3), describes the relationship between KPC variations and KCC input variations ($\mathbf{Y}(N)$ and $\mathbf{U}(k)$ and their covariance matrices $\mathbf{K}_Y$ and $\mathbf{K}_U$ in equation (4)). The potential evaluation index, namely, the ratio of KPC variations over KCC variations can be expressed in terms of the model matrix $\boldsymbol{\gamma}(k)$. (ii) The process design information is embedded in system matrices $\mathbf{A}$, $\mathbf{B}$, and $\mathbf{C}$, which are determined by the station-to-station locating layout change, the geometry of fixture locating layout on individual stations, and the selection of KPCs, respectively. The model matrix $\boldsymbol{\gamma}(k)$ incorporates design information included in those system matrices. In

short, the aforementioned two items (i) and (ii) imply that the state space model integrates rich process design information, serving as the basis for the development of desirable design evaluation indices. The evaluation of multistation assembly process design can then be conducted parallel to the sensitivity analysis of a dynamic system.

A single design evaluation index is inadequate to describe critical aspects of variation propagation in a multistation assembly system. The index based on the entire system variation input and output characterizes the overall process performance, however, it does not provide any detailed information about an individual station or a single fixture. On the other hand, the index based on the variation input and output of a single fixture characterizes the performance of a single fixture during production, but it does not provide the joint effect of multiple variation inputs at the system level. Therefore, a group of hierarchical multilevel indices is developed to capture critical aspects of the variation behavior of a multistation assembly process. Furthermore, these multilevel indices are expressed in terms of critical process design characteristics and are independent of variation inputs since it is the design configuration that needs to be evaluated rather than the transmitted variation as it was presented in section 4.1.

For the N-station assembly process shown in Figure 12, the KPC variation is denoted as a variance vector, σ^2_{output}, with elements that are the diagonal elements of $\mathbf{K}_Y$, i.e., $\sigma^2_{\text{output}} = \text{diag}(\mathbf{K}_Y)$. The KCC variation inputs are decomposed into three levels. Variation σ^2_{kp} at the single fixture level stands for the variance of the pth locating feature at station k. Variation vector σ^2_k at a single station level is denoted as

$$\sigma^2_k = \left[\sigma^2_{k1} \cdots \sigma^2_{kp} \cdots \sigma^2_{km_k}\right]^{\mathrm{T}}.$$

It is easy to verify that $\sigma^2_k = \text{diag}(\mathbf{K}_p(k))$. Variation vector σ^2_{input} represents the variation inputs of the entire process and is defined as

$$\sigma^2_{\text{input}} = \left[\sigma^{2^{\mathrm{T}}}_1 \cdots \sigma^{2^{\mathrm{T}}}_k \cdots \sigma^{2^{\mathrm{T}}}_N\right]^{\mathrm{T}}.$$

The sensitivity analysis for design evaluation defines: (1) how the system responds to certain variation inputs; (2) which variation source contributes most to the final product variation; and/or (3) how related process parameters account most for the variation propagation. As such, the sensitivity indices are similar to the system gains in control theory. Appropriate measure is introduced to represent process sensitivity as the gain of a multiple-input-multiple-output (MIMO) system. Three-level sensitivity indices are defined to facilitate the description of the system behavior of a multistation assembly process: single fixture level, station level with multiple fixtures, and system level (multistation).

The design evaluation index (DEI) at the fixture level, denoted as S_{kp}, is defined as

$$S_{kp} = \frac{\left\|\mathbf{W}\sigma^2_{\text{output}}\right\|_2}{\sigma^2_{kp}}. \tag{15}$$

where weighting coefficient $\mathbf{W}$ determines the relative importance of KPC variances and $\|\cdot\|_2$ is the Euclidean norm. S_{kp} index indicates how the pth locating feature at station k contributes to the KPC variations. In fact, at this level, S_{kp}, corresponds to the gain of a Single-Input-Multiple-Output (SIMO) system.

The DEI at the station level, denoted as S_k, is defined as

$$S_k = \sup_{\sigma_k^2} \frac{\|\mathbf{W}\sigma_{\text{output}}^2\|_2}{\|\sigma_k^2\|_2}. \tag{16}$$

S_k index indicates how the fixture elements on station k jointly affect the KPC variation. It is a MIMO-type gain since each station contains multiple fixtures. Station-level sensitivity index S_k identifies the critical station contributing most to the KPC variation.

The DEI at the system level, denoted as S_o, is defined as

$$S_o = \sup_{\sigma_{\text{input}}^2} \frac{\|\mathbf{W}\sigma_{\text{output}}^2\|_2}{\|\sigma_{\text{input}}^2\|_2} \tag{17}$$

S_o index indicates the system capacity to amplify or suppress the input variations. S_o index is also a MIMO-type gain.

The aforementioned defined indices S_{kp}, S_k, and S_o are the ratios of KPC variation over the KCC variation. Consider $\|\mathbf{W}\sigma_{\text{output}}^2\|_2$ as the indicator of KPC variation level. Indices S_{kp}, S_k, and S_o are the values of KPC variation given a unit KCC variation input. The unit of KCC variation is different for the three indices: for a single fixture, a unit KCC variation is equivalent to $\sigma_{kp}^2 = 1$; for a station, a unit KCC variation is the joint effect from the multiple fixtures, defined as $\|\sigma_k^2\|_2 = 1$; for the entire system, a unit KCC variation is the combined effect from the multiple stations, defined as $\|\sigma_{\text{input}}^2\|_2 = 1$. A sensitivity index less than 1 means that the KPC variation level can become lower than the KCC variation level. On the contrary, a sensitivity index larger than 1 implies that the system amplifies the input variation. Most of the multistation systems will end up with a sensitivity greater than 1. Nonetheless, a smaller sensitivity value suggests a less variation-sensitive system which is preferable. Therefore, using and comparing this group of indices, a robust process configuration can be selected and the sensitive station and fixture can be identified and prioritized.

Next, the indices S_{kp}, S_k, and S_o are expressed in terms of the model matrix γ so that they are made input independent.

It has been proved that if the KCC variation inputs in Figure 11 are uncorrelated, the KPC variance vector σ_{output}^2 can be represented as a linear combination of the vector σ_k^2. The expression can be represented as

$$\sigma_{\text{output}}^2 = \sum_{k=1}^{N} [\gamma^2(k)] \cdot \sigma_k^2 \tag{18}$$

where $[\gamma^2(k)]$ represents a matrix in which each element is the square of the corresponding element in matrix $\gamma(k)$, i.e.,

$$[\gamma^2] = \begin{bmatrix} \gamma_{11}^2 & \gamma_{12}^2 & \cdots & \gamma_{1m}^2 \\ \gamma_{21}^2 & \gamma_{22}^2 & \cdots & \gamma_{2m}^2 \\ \vdots & \vdots & \ddots & \vdots \\ \gamma_{q1}^2 & \gamma_{q2}^2 & \cdots & \gamma_{qm}^2 \end{bmatrix}. \tag{19}$$

According to the definition of S_{kp} index, it is assumed that there is only a single variation source (rather than multiple simultaneous sources) in the entire process at each time.

The fixture-level sensitivity index S_{kp} for the pth KCC on station k can be proved (Ding et al., 2002a) to be

$$S_{kp} = \left\| \mathbf{W} \cdot \gamma_p^2(k) \right\|_2 \tag{20}$$

The second index is the station sensitivity index S_k. It is assumed that only one station has variation inputs at a time. But within each station, more than one fixture element could contribute to σ_{output}^2 simultaneously.

The station-level sensitivity index S_k can be expressed as Ding et al. (2002a)

$$S_k = \| \mathbf{W} \cdot [\gamma^2(k)] \|_2. \tag{21}$$

System-level sensitivity will consider all possible combinations of multiple KCC variation inputs—within a station and/or cross-stations. Thus, it represents the overall sensitivity level of a process as to the KCC variation inputs.

The system-level sensitivity index S_o can be expressed as Ding et al. (2002a)

$$S_o = \| \mathbf{W} \cdot [\gamma^2(1)\gamma^2(2) \cdots \gamma^2(N)] \|_2. \tag{22}$$

It is also possible to define the station and system sensitivity indices using the fixture sensitivity index, that is, choosing the largest fixture sensitivity index within a station or in a process as the station and system indices, respectively. Under this definition, these new indices could represent process response to a single variation input, whereas the proposed indices (equations (16) and (17)) describe the joint effect of multiple simultaneous variation inputs. The results are different using the two sets of definitions. The selection between both sets of indices depends on the specific requirements of applications.

Case study.   The assembly process of the sport utility vehicle (SUV) side panel is used to illustrate the concepts of sensitivity analysis and demonstrate the design evaluation methodology. In addition to KCCs P_1–P_8 used in the assembly process, there is an extra locating hole P_9 (Figure 19) on the rear quarter panel which can be used to first position
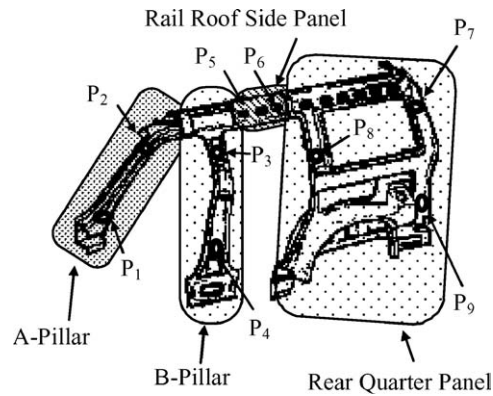
Figure 19. KCCs P_1–P_9 on the assembly.

this panel on station III, and then the whole subassembly on the measurement station. The nominal design positions of the fixture locators (KCCs) and KPC points in 2D (X–Z coordinates) are given in Tables 5 and 6, respectively.

Four alternative process configuration schemes marked as C1–C4 are used for evaluation. Configuration C1 is currently used in one US automotive assembly plant and is utilized here as the reference in our design evaluation. A major difference between other configurations (C2, C3, C4) and C1 is that locator P_9 is used to replace P_7 when the rear quarter panel is located on station III. The fixture locating layout for each configuration is presented in Table 7.

In order to evaluate the different design configurations, a state space model is developed for the above four configurations, following methods presented in Jin and Shi (1999) and Ding, et al. (2000). The sensitivity-based design evaluation is then conducted following the

Table 5. Coordinates of fixture locators (KCCs) from Figure 19 (units: mm).

KCC	P_1	P_2	P_3	P_4	P_5
(X, Z)	(367.8,906.05)	(667.47,1295.35)	(1301,1368.89)	(1272.73,537.37)	(1470.71,1640.40)
KCC	P_6	P_7	P_8	P_9	
(X, Z)	(1770.50,1702.62)	(2941.42,1691.31)	(2120.32,1402.83)	(3026.25, 950.30)	

Table 6. Coordinates of KPCs from Figure 20(d) (units: mm).

KPC	M_1	M_2	M_3	M_4	M_5
(X, Z)	(271.50,905)	(565.7, 1634.7)	(1289.7,1227.5)	(1306.5,633.5)	(1244.5,85)
KPC	M_6	M_7	M_8	M_9	M_{10}
(X, Z)	(1604.5,1781.8)	(2884.8,1951.5)	(2743.5,475.2)	(1838.4,226.3)	(1979.8,1459.4)

Table 7. Process configuration schemes.

Configuration	Assembly Sequence
C1	$\{\{P_1, P_2\}, \{P_3, P_4\}\}_I \rightarrow \{\{P_1, P_4\}, \{P_5, P_6\}\}_{II} \rightarrow \{\{P_1, P_6\}, \{P_7, P_8\}\}_{III} \rightarrow \{\{P_1, P_8\}\}_{IV}$
C2	$\{\{P_1, P_2\}, \{P_3, P_4\}\}_I \rightarrow \{\{P_1, P_4\}, \{P_5, P_6\}\}_{II} \rightarrow \{\{P_1, P_6\}, \{P_8, P_9\}\}_{III} \rightarrow \{\{P_1, P_9\}\}_{IV}$
C3	$\{\{P_1, P_2\}, \{P_4, P_3\}\}_I \rightarrow \{\{P_4, P_2\}, \{P_5, P_6\}\}_{II} \rightarrow \{\{P_4, P_6\}, \{P_8, P_9\}\}_{III} \rightarrow \{\{P_4, P_9\}\}_{IV}$
C4	$\{\{P_1, P_2\}, \{P_4, P_3\}\}_I \rightarrow \{\{P_4, P_2\}, \{P_5, P_6\}\}_{II} \rightarrow \{\{P_1, P_6\}, \{P_8, P_9\}\}_{III} \rightarrow \{\{P_1, P_9\}\}_{IV}$

three steps. During this case study, the weight coefficient matrix **W** is selected as an identity matrix, implying that all KPCs are treated with equal importance.

Step 0: State space modeling of the assembly process.   In this SUV side panel assembly process, there are three assembly stations and one inspection station, i.e., $N = 4$ (see Figure 20). The fixture used on the inspection station is considered well maintained and calibrated with much higher repeatability than those on a regular assembly station. Thus, the input variation of fixture locators on the measurement station is neglected and the KCC
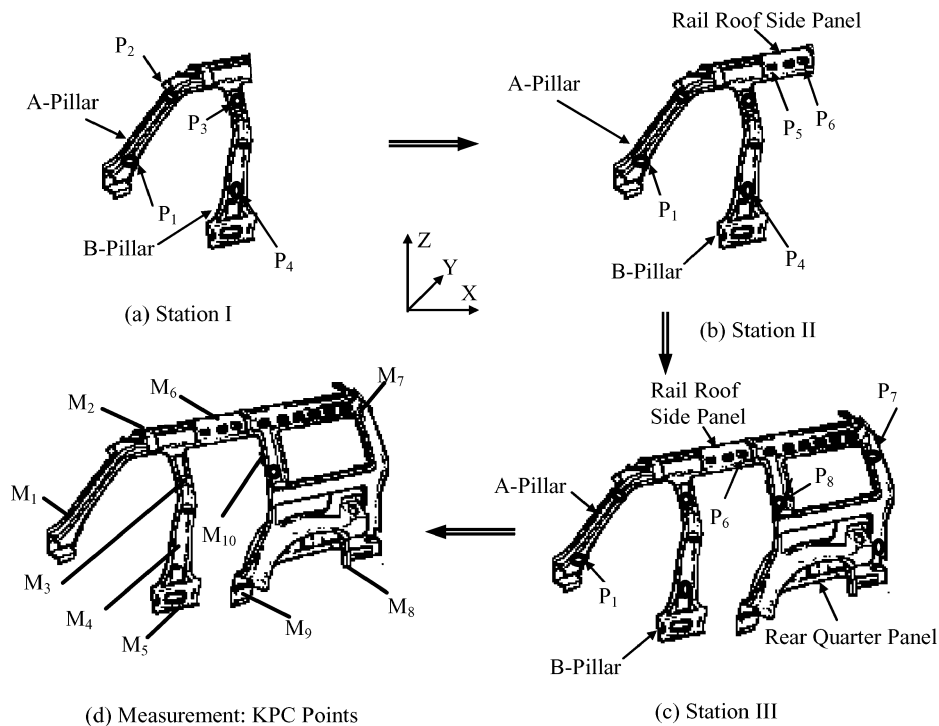

(a) Station I

(b) Station II

(c) Station III

(d) Measurement: KPC Points

Figure 20.   Assembly process of the side aperture panel of a SUV.

Table 8. Process sensitivity index for C1–C4 process configuration.

	C1	C2	C3	C4
S_o	6.14	3.33	3.26	3.13

deviation inputs from fixtures on three assembly stations, U(1), U(2), and U(3), are included. The design evaluation is conducted to benchmark the three assembly stations. A state space model can be set up for this SUV side panel assembly process as

$$
\begin{cases}
\mathbf{X}(1) = \mathbf{B}(1)\mathbf{U}(1) + \mathbf{W}(1) \\
\mathbf{X}(k) = \mathbf{A}(k-1)\mathbf{X}(k-1) + \mathbf{B}(k)\mathbf{U}(k) + \mathbf{W}(k), \ k = 2, \ 3 \\
\mathbf{X}(4) = \mathbf{A}(3)\mathbf{X}(3) + \mathbf{W}(4) \\
\quad \mathbf{Y} = \mathbf{C}\mathbf{X}(4) + \mathbf{V}
\end{cases}
\tag{23}
$$

where $\mathbf{A}$s, $\mathbf{B}$s, and $\mathbf{C}$ can be obtained by substituting the parameters given in Tables 5 and 6 to equations (38), (39), and (45) in Jin and Shi (1999).

Step 1: System level design evaluation. The system sensitivity indices regarding all four process configurations are calculated and presented in Table 8.

It is known that the lower the index value, the better the robustness of a process design. Comparing two sensitivity indices, we further quantify the significance of improvement (SOI) as

$$
\text{SOI} = \frac{S_o^{\text{old}} - S_o^{\text{new}}}{S_o^{\text{old}}}\%.
\tag{24}
$$

SOI represents the percentage of KPC variation level change given a unit KCC variation input when a new process design configuration is compared to the original design configuration. A negative SOI means that the process sensitivity actually increases and the system robustness deteriorates. The value range of a SOI to be significant depends on the trade off between the savings from quality improvement and the efforts in making the changes. The determination of quantitative SOI significant range could be conducted only where the following relations are known: (a) statistical distributions of KPC/KCC variables, (b) tolerance limits, and (c) variation/tolerance versus cost (scrap, rework, warranty etc.). In the presented case study, based on our industrial knowledge and discussions with automotive engineers, we consider the SOI greater than 20% as significant, between 10 and 20% as marginally significant, and less than 10% as insignificant.

One can calculate based on Table 8 that SOI $= 45\%$–49% when either one of the configurations C2, C3, and C4 is compared with C1, the current industrial configuration. It is concluded that the sensitivity level drops considerably when P_9 is used to replace P_7. The new configuration with P_9 significantly improves the system's robustness. The result suggests that C1, the design configuration currently used in industry, is not the optimal one with respect to the system robustness to dimensional variations. However, the SOI between

Table 9. Station sensitivity index for configuration C4.

	Station I	Station II	Station III
S_k	2.94	1.69	3.01

any two of the other three process designs using P_9 (options C2, C3, and C4) is smaller than 6%. Therefore, their differences are not significant. The fourth scheme (C4) yields the lowest S_o value among the four process configurations. The value of SOI equals 49.0% when C4 is compared with C1, which corresponds to a 49.0% decrease in KPC variation level under the same condition of KCC variation input. Hence, it is recommended that the current process design should be replaced by configuration C4.

Step 2: Station level design evaluation.   Let us further study the station sensitivity of the C4 configuration to identify which station has the largest contribution towards the KPC variation. Sensitivity indices for three stations are shown in Table 9. The percentage of variation contribution (PVC) from station k can be calculated using the following index

$$\text{PVC}_k = \frac{S_k}{\Sigma_{k=1}^{N} S_k} \%. \tag{25}$$

One can find that $\text{PVC}_3 = 39.4\%$, $\text{PVC}_1 = 38.5\%$, and $\text{PVC}_2 = 22.1\%$. The third and most critical station produces the highest sensitivity and PVC value. Station I also has remarkable contribution to the KPC variation. Stations I and III together account for 77.9% contribution in the KPC variation level. Station II has the lowest station sensitivity and the smallest PVC value. It would be the designer's highest priority to investigate the design layouts of stations I and III.

Step 3: Fixture level design evaluation.   Finally, the fixture sensitivity index is computed for evaluation. At each station, four independent locating pins position two parts/subassemblies. The total 12 indices are shown in Table 10.

From the above table, it can be ascertained that not all locators at station II are major variation contributors. Stations I and III include certain critical variation sources. Locators

Table 10. Fixture sensitivity index for configuration C4.

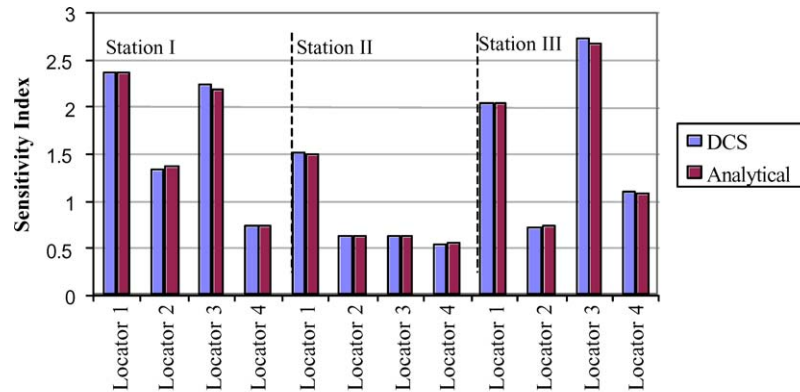|	Station I	Station II	Station III
Locator 1	2.38	1.50	2.03
Locator 2	1.37	0.69	0.75
Locator 3	2.18	0.65	2.68
Locator 4	0.75	0.56	1.09

Figure 21. Comparison of sensitivity index from DCS and analytical approach.

1 and 3 (4-way locators) at stations I and III cause the largest variations in the final assembly if the input variations have the same magnitude. The variation reduction and design effort should be first focused on stations I and III to reduce the sensitivity of these two 4-way locators.

A numeric variation simulation analysis software based on the Monte Carlo (DCS, 2000) can be used to obtain the sensitivity indices. As discussed earlier in this section, it is difficult and time consuming to compute MIMO-type of indices such as S_k and S_o using DCS. Thus, the DCS software is only used to obtain the fixture level sensitivity index S_{kp}. An identical assembly process as presented in the case study is modeled using the VSL language and the numerical variation model is generated in the DCS. A normal variation source with $3\sigma = 1$ is assigned to one fixture locator each time, and 5000-run Monte Carlo simulations are then conducted. The sensitivity index is computed by dividing the KPC variation by the input source's variance. The results are compared with those values in Table 10, which are calculated from design parameters using analytical formulations. The comparison is shown in Figure 21, where we can observe good consistency between the analytical and numerical calculations of fixture level sensitivity index. The maximum difference is less than 3.2%.

5. Conclusions

Currently, a new paradigm is emerging in manufacturing and design in which increased customization, product proliferation, heterogeneous markets, shorter product life cycle and development time, responsiveness etc. are increasingly taking center stage. One of the characteristic features of the modern manufacturing and new product development in automotive, aerospace, and other industries is the frequency of model change and the vast amounts of time and cost required to make a changeover, also called time-based competition. This trend has continuously gone up in the last two decades.

A major obstacle in effective time-based competition is the often costly, difficult and time-consuming identification of root causes of the stream of variation (dimensional variation propagation) in complex multistage manufacturing systems.

This paper discusses the concept of time-based competition in manufacturing and design based on the review of on-going research related to stream-of-variation (SOVA) methodology. The presented methodology is based on the state space model characterizing variation propagation in a multistage process. The state space model describes a discrete-time LTV (linear time varying) stochastic system, which strongly indicates that the existing system and control theory could be used to perform systematic analysis and achieve variation control of the manufacturing process. Moreover, the state space model integrates information of product quality with process information such as tooling status, therefore, providing the basis for fault diagnosis. The model is validated through simulation comparison with the widely used variation simulation software 3DCS (DCS, 2000). The applications of the presented SOVA model for dimensional fault diagnostics, design evaluation, and sensor placement are presented.

While the presented research is conducted within the context of automotive assembly process, the methodology is applicable to generic multistage manufacturing processes.

Acknowledgments

References

Apley, D. W. and Shi, J., "Diagnosis of Multiple Fixture Faults in Panel Assembly," *ASME Journal of Manufacturing Science and Engineering*, Vol. 120, pp. 793–801 (1998).

Baron, J., "Dimensional Analysis and Process Control of Body-In-White Processes," Ph. D. Dissertation, University of Michigan, Ann Arbor, MI (1992).

Bollinger, J. E. (Ed.), *Visionary Manufacturing Challenges for 2020*, Committee on Visionary Manufacturing Challenges, National Research Council, National Academy Press, Washington, DC (1998).

Cai, W., Hu, S. J., and Yuan J. X., "Deformable Sheet Metal Fixturing: Principles, Algorithms, and Simulations," *Transactions of ASME, Journal of Manufacturing Science and Engineering*, Vol. 118, No. 3, pp. 318–324 (1996).

Camelio, J., Hu, S. J., and Ceglarek, D., "Modeling Variation Propagation of Multi-Station Assembly Systems with Compliant Parts," *Transactions of ASME, Journal of Mechanical Design*, Vol. 125, No. 4, pp. 673–681 (2003).

Ceglarek, D., "Knowledge-Based Diagnosis for Automotive Body Assembly: Methodology and Implementation," Ph.D. Dissertation, University of Michigan, Ann Arbor, MI (1994).

Ceglarek, D. and Shi, J., "Dimensional Variation Reduction for Automotive Body Assembly Manufacturing," *Manufacturing Review*, Vol. 8, No. 2, pp. 139–154 (1995).

Ceglarek, D. and Shi, J., "Fixture Failure Diagnosis for Auto Body Assembly Using Patter Recognition," *ASME Transactions, Journal of Engineering for Industry*, Vol. 118, No. 1, pp. 55–65 (1996).

Ceglarek, D. and Shi, J., "Design Evaluation of Sheet Metal Joints for Dimensional Integrity," *Transactions of ASME, Journal of Manufacturing Science and Engineering*, Vol. 120, No. 2, pp. 452–460 (1998).

Ceglarek, D., Shi, J., and Wu, S. M., "A Knowledge-Based Diagnosis Approach for the Launch of the Auto-Body Assembly Process," *Transactions of ASME, Journal of Engineering for Industry*, Vol. 116, No. 4, pp. 491–499 (1994).

Chase, K. W. and Parkinson, A. R., "A Survey of Research in the Application of Tolerance Analysis to the Design of Mechanical Assemblies," *Res. Eng. Design*, Vol. 3, pp. 23–37 (1991).

CIRP, "Flexible Automation—Assessment and Future," *CIRP Scientific Technical Committee Survey in USA, Europe and Japan* (January 27, 2000).

DCS, *3D Variation Simulation*, Dimensional Control Systems, Inc. (2000).

Ding, Y., Ceglarek, D., and Shi, J., "Modeling and Diagnosis of Multistage Manufacturing Process: Part I State Space Model," *Proceedings of 2000 Japan–USA Symposium on Flexible Automation*, July 23–26, Ann Arbor, MI, 2000JUSFA-13146 (2000).

Ding, Y., Ceglarek, D., and Shi, J., "Design Evaluation of Multi-station Assembly Processes by Using State Space Approach," *ASME Transactions, Journal of Mechanical Design*, Vol. 124, No. 3, pp. 408–418 (2002a).

Ding, Y., Ceglarek, D., and Shi, J., "Fault Diagnosis of Multistage Manufacturing Processes by Using State Space Approach," *ASME Transactions, Journal of Manufacturing Science and Engineering*, Vol. 124, No. 2, pp. 313–322 (2002b).

Ding, Y., Shi, J., and Ceglarek, D., "Diagnosability Analysis of Multistage Manufacturing Processes," *ASME Transactions, Journal of Dynamic Systems, Measurement, and Control*, Vol. 124, No. 1, pp. 1–13 (2002c).

Ding, Y., Kim, P., Ceglarek, D., and Jin, J., "Optimal Sensor Distribution for Variation Diagnosis in Multi-Station Manufacturing Processes," *IEEE Transactions on Robotics and Automation*, Vol. 19, No. 4, pp. 543–556 (2003).

El-Gizawy, A. S., Hwang, J.-Y., and Brewer, D. H., "A Strategy for Integrating Product and Process Design of Aerospace Components," *Manufacturing Review*, Vol. 3, No. 3, pp. 178–186 (1990).

ERC-RMS, National Science Foundation–Engineering Research Center for Reconfigurable Manufacturing Systems (ERC-RMS), Technical Report, University of Michigan (1999).

Gadh, R., "A Hybrid Approach to Intelligent Geometric Design Using Features-Based Design and Feature Recognition," *Proceedings of the 19th Annual ASME Design Automation Conference*, Vol. DE-65, No. 2, pp. 273–283 (1993).

Gerwin, D. and Barrowman, N. J., "An Evaluation of Research on Integrated Product Development," *Management Science*, Vol. 48, No. 7, pp. 938–953 (2002).

Greer, D., "On-line Machine Vision Sensor Measurements in a Coordinate System," SME Paper #IQ88–289 (1988).

Hu, S. J., "Impact of 100% Measurement Data on Statistical Process Control (SPC) in Automobile Body Assembly," Ph.D. Dissertation, University of Michigan, Ann Arbor, MI (1990).

Hu, S. J., "Stream-of-Variation Theory for Automotive Body Assemblies," *Annals of CIRP*, Vol. 46, No. 1, pp. 1–6 (1997).

Hu, S. and Wu, S. M., "Identifying Root Causes of Variation in Automobile Body Assembly Using Principal Component Analysis," *Transactions of NAMRI*, Vol. 20, pp. 311–316 (1992).

Huang, W., Kong, Z., Ceglarek, D., and Brahmst, E., "The Analysis of Feature-Based Measurement Error in Coordinate Metrology," *IIE Transactions on Design and Manufacturing*, Vol. 36, No. 3, pp. 237–251 (2004).

Jin, J. and Shi, J., "State Space Modeling of Sheet Metal Assembly for Dimensional Control," *ASME Transactions, Journal of Manufacturing Science & Engineering*, Vol. 121, pp. 756–762 (1999).

Khan, A., Ceglarek, D., and Ni, J., "Sensor Location Optimization for Fault Diagnosis in Multi-Fixture Assembly Systems," *Transactions of ASME, Journal of Manufacturing Science and Engineering*, Vol. 120, No. 4, pp. 781–792 (1998).

Khan, A., Ceglarek, D., Shi, J., Ni, J., and Woo, T. C., "Sensor Optimization for Fault Diagnosis in Single Fixture Systems: A Methodology," *ASME Transaction, Journal of Manufacturing Science and Engineering*, Vol. 121, pp. 109–117 (1999).

Koren, Y., Heisel, U., Jovane, F., Moriwaki, T., Pritschow, G., Ulsoy, G. A., and Brussel, H., "Reconfigurable Manufacturing Systems," *Annals of CIRP*, Vol. 50, No. 2 (1999).

Lawless, J. F., Mackay, R. J., and Robinson, J. A., "Analysis of Variation Transmission in Manufacturing Processes—Part I," *Jouranal of Quality Technology*, Vol. 31, pp. 131–142 (1999).

Mantripragada, R. and Whitney, D. E., "Modeling and Controlling Variation Propagation in Mechanical Assemblies Using State Transition Models," *IEEE Transactions on Robotics and Automation*, Vol. 15, pp. 124–140 (1999).

Mehrabi, M. G., Ulsoy, A. G., and Koren, Y., "Reconfigurable Manufacturing Systems: Key to Future Manufacturing," *Journal of Intelligent Manufacturing*, Vol. 11, No. 4, pp. 403–419 (2000).

Menassa, R. J. and DeVries, W. R., "Locating Point Synthesis in Fixture Design," *Annals of CIRP*, Vol. 38, No. 1, pp. 165–169 (1989).

Parkinson, A., Sorensen, C., and Pourhassan, N., "A General Approach for Robust Optimal Design," *Transactions of ASME, Journal of Mechanical Design*, Vol. 115, No. 1, pp. 74–80 (1993).

Perceptron, 1000, "Measurement System Manual," Perceptron Inc. (1991).

Sekine, Y., Koyama, S., and Imazu, H., "Nissan's New Production System: Intelligent Body Assembly System," SAE Technical Paper Series, 910816, pp. 1–12 (1991).

Shalon, D., Gossard, D., Ulrich, K., and Fitzpatrick, D., "Representing Geometric Variations in Complex Structural Assemblies on CAD Systems," *Proceedings of the 19th Annual ASME Advances in Design Automation Conference*, Vol. DE-44, No. 2, pp. 121–132 (1992).

Suri, R., *Quick Response Manufacturing: A Company wide Approach to Reducing Lead Times*, Productivity Press (1998).

Takezawa, N., "An Improved Method for Establishing the Process-Wise Quality Standard" *Rep. Stat. Appl. Res.*, JUSE, Vol. 27, No. 3, pp. 63–75 (1980).

Thomke, S. and Fujimoto, T., "The Effect of "Front-Loading" Problem-Solving on Product Development Performance," *Journal of Production Innovation Management*, Vol. 17, No. 2, pp. 128–142 (2000).

Ulrich, K., Sartorius, D., Pearson, S., and Jakiela, M., "Including the Value of Time in Design-for-Manufacturing Decision-Making," *Management Science*, Vol. 39, No. 4, pp. 429–447 (1993).